

A systematic investigation on the effects of temperature and relative humidity on the performance of eight low-cost particle sensors and devices

Yangyang Zou, Jordan D. Clark, Andrew A. May *

Department of Civil, Environmental, and Geodetic Engineering, The Ohio State University, USA



ABSTRACT

Low-cost particle sensors are rapidly gaining popularity for indoor air quality monitoring, but their accuracy has been shown to vary among products and among environments in which they operate. Previous research has explored the effect of environmental conditions including temperature and humidity on sensor accuracy and found appreciable effects of these variables in many cases. We extend this work to cover some models that have not been previously tested and analyze results in a way to establish the significance of environmental variables on low-cost sensor output. In this study, we conduct a series of laboratory experiments in which temperature and relative humidity (RH) are varied in a precisely controlled chamber and different common particle sources introduced. Eight different brands of low-cost particle sensors, some of which have not been previously analyzed in this manner, measured particle concentration inside the chamber and were compared to research-grade instruments. Comparison of the output of the research-grade instruments with that of the low-cost sensors yielded a few interesting results. First, temperature showed no statistically significant effect on sensor performance in any case, at 99% confidence. Second, RH appears to affect the magnitude of low-cost sensor output but not its correlation to research-grade instruments output, suggesting the possibility of RH-based calibration.

1. Introduction

One promising area within the field of smart buildings is in smart monitoring, maintenance, and control of indoor environments. Low-cost air quality sensors can conceivably be used to ensure optimal operation of building air quality control systems and enable decision making based on reliable monitoring data. Chief among the airborne pollutants of interest for monitoring with these sensors is airborne particulate matter (PM). The link between PM exposure and numerous negative health outcomes is well established. Exposure to PM is linked to cardiovascular and respiratory disease, and the majority of this exposure occurs indoors for Westerners, as this is where we spend the vast majority of our time (Klepeis et al., 2001). Indoor sources of PM include combustion activities, outdoor penetration, mold, and airborne formation from gases emitted from cleaning products, furniture, or other building products (Li, Wen and Zhang 2017).

Numerous low-cost particle sensors have become commercially available recently for as little as \$10 (US dollars) and may provide an inexpensive means to help assess and control PM exposure. These sensors usually consist of a light source (typically, a small LED) that is scattered by a stream of particles passing by it, and a small photoreceptor receiving this scattered light signal. Researchers have conducted many investigations of one or more aspects of the performance of these sensors, and mechanisms for deviation in performance from that of more expensive research-grade instruments have been identified. One of these mechanisms is the changes that occur at different psychrometric conditions.

* Corresponding author.

E-mail address: may.561@osu.edu (A.A. May).

There is little evidence that temperature has a substantial effect on the accuracy of low-cost sensors, within a reasonable range of temperatures, despite the fact that some sensors introduce air into the sensor via thermally-induced buoyancy via a resistive heater located within the sensor. [Budde, El Masri, Riedel, and Beigl \(2013\)](#) noted a correlation between the output from a Sharp GP2Y sensor, which utilizes buoyancy-driven air, and temperature when each instance (one instance equals one unique unit of the same sensor model; multiple instances were tested in the study) of the sensor was held at a constant concentration of $0 \mu\text{g m}^{-3}$, but this effect was slight. [Zamora et al. \(2019\)](#) conducted field and laboratory evaluations of the low-cost Plantower PMS A003 sensor, which contains a small internal fan to drive air flow, and found no observable effect of temperature on low-cost particle sensor performance.

With regards to airborne moisture, however, several studies concluded that relative humidity (RH) has an impact on sensor performance. [Badura, Batog, Drzeniecka-Osiadacz, and Modzel \(2018\)](#) suggested four mechanisms may be responsible: hygroscopic growth leading to changes in particle diameter ([Crilley et al., 2018](#)); changes in the refractive index of particles, which can affect light scattering; moisture interference with electrical components, up to and including failure ([Wang et al., 2015](#)) and scattering of sensor LED light by moisture itself, which may occur at extreme RH ([Jayaratne, Liu, Thai, Dunbabin, & Morawska, 2018](#)).

Several laboratory studies have measured relationships between RH and sensor output. [Zamora et al. \(2019\)](#) discovered that the accuracy of Plantower PMS A003 decreased at RH greater than 50%. [Wang et al. \(2015\)](#) found that the Sharp GP2Y sensor output increased as RH increased. Similar phenomena have been measured in the field. [Han, Symanski, and Stock \(2017\)](#) observed that the PM2.5 and PM10 concentration were correlated to RH. [Feeenstra et al. \(2019\)](#) found increasing positive bias error for 12 particle sensors during field base monitoring as RH increased. [Liu, Schneider, Haugen, and Vogt \(2019\)](#) also noticed increase of sensor error at higher RH level (greater than 80% RH) for outdoor particle monitoring. [Jayaratne et al. \(2018\)](#) observed that the Plantower PMS1003 mass concentration increased by 80% with RH increase from 78 to 89% during field monitoring. In general, these studies all provide evidence that sensor output depends on RH.

In contrast, several studies concluded that neither temperature nor RH affect sensors' performance. [Badura et al. \(2018\)](#) tested 5 sensors in outdoor environments with temperatures ranging from -8°C to $+36^\circ\text{C}$ and RH ranging from 27% to 94% but found no effect. [Malings et al. \(2020\)](#) found little RH effect and attributed this to the plastic shell, which enclosed their sensors, trapping heat and reducing RH. [Bulot et al. \(2019\)](#) found that neither RH nor temperature had an influence on performance of multiple sensors in a school.

With these previous studies in mind, we conducted a series of experiments by varying temperature and humidity in a precisely controlled chamber, with eight different brands of low-cost particle sensors, some of which have not yet been tested in publicly available studies. Our primary objective in these investigations was to quantify the relationship between temperature and RH for the range expected in building applications and the output of eight low-cost sensor models (relative to research-grade instruments), some of which have not been previously analyzed in this manner.

2. Methodology

2.1. Sensors tested

We tested three bare sensors and five integrated devices. We define bare sensors as small sensors, usually less than 10 cm along their longest edge, which output an electrical signal (analog or digital), that then must then be translated into something understandable by its users and/or by other devices. The bare sensors we are testing are exclusively optical sensors. Bare sensors tested as well as relevant specifications are given in [Table 1](#). We refer to bare sensors as "BS" from here forward. Multiple instances were tested for each type of BS as shown in [Table 1](#).

We refer to packaged devices that utilize bare sensors and fulfill the necessary conversion from raw sensor outputs to produce concentrations as "integrated devices". Many also offer built-in features such as Bluetooth or Wi-Fi connectivity, SD card storage, temperature and relative humidity sensors, other pollutant sensors, and/or compatibility with other smart devices like thermostats. Most of the integrated devices targeted towards residential consumers fall into the \$200 – \$300 (US dollars) price range. Bare sensors are incorporated into each of the integrated devices we are also testing. Specifications for the integrated devices tested are given in [Table 2](#). We refer integrated devices as "ID" from here forward. Multiple instances were tested for each type of ID except for ID1, as shown in [Table 2](#).

2.2. Experimental setup

We subjected each of these sensors as well as research-grade instruments to particle sources in a series of environmental conditions and particle sources. A schematic of the experimental setup is shown in [Fig. 1](#). The low-cost sensors were placed inside a chamber with dimensions of 46" (L) x 62" (W) x 35" (H) ($1.17 \text{ m} \times 1.57 \text{ m} \times 0.89 \text{ m}$), built out of 4" (0.10 m) thick rigid insulation, labeled "Testing Chamber" in [Fig. 1](#). These sensors were elevated on wire racks to allow adequate airflow around them, similar to the setup in [Zou, Young, Chen, et al. \(2020\)](#). A photograph of the interior of the testing chamber (insulation chamber) is given in [Fig. 2](#). Throughout all experiments, air was drawn from the testing chamber by our research-grade instruments: a TSI Scanning Mobility Particle Sizer (SMPS) Model 3938, which included a Model 3081 long DMA and a model 3775 Condensation Particle Counter (CPC); and a TSI Aerodynamic Particle Sizer (APS) Model 3321, as in previous work ([Zou, Young, Chen, et al., 2020; Zou, Young, Wickey, et al., 2020](#)).

Because water uptake by the particles at elevated RH will increase the particle diameter, particle mass concentrations will increase. To enable a direct comparison of the quantified concentrations of these "wet" particles by both the sensors and the research-grade instruments, we did not dry the particles prior to detection by the SMPS and APS. In other words, the growth of particles due to

Table 1

Information related to the bare sensors included in this study.

Sensor	Cost (US dollars)	Intake	Manufacturer	Use in Integrated Sensor(s)	Intended Indoor Environment	Previous Studies	No. of Units Tested	LB ($\mu\text{g m}^{-3}$)	UB ($\mu\text{g m}^{-3}$)
Honeywell HPMA115S0 (BS1)	~\$30	Fan	0–1000 $\mu\text{g m}^{-3}$	None	Air conditioners, air quality monitors, environmental monitoring, air cleaners, air quality detectors	Bulot et al. (2020)	2	8.42	628
Sharp GP2Y1010AU0F (BS2)	~\$12	Resistor	0–500 $\mu\text{g m}^{-3}$	Foobot, AirAssure, UB Air Sense	Detecting dust in air, air purifier, air conditioner, air monitors, and distinguishing between smoke and house dust	Budde et al. (2013) Weekly et al. (2013)* Wang et al. (2015) Hojaiji, Kalantarian, Bui, King, and Sarrafzadeh (2017) Liu et al. (2017), Sousan, Koehler, Hallett, and Peters (2016)	3	12.43	2205
Plantower PMS5003 (BS3)	~\$30	Fan	Effective: 0–500 $\mu\text{g m}^{-3}$ Maximum: 0–1000 $\mu\text{g m}^{-3}$	TSI Bluesky, Purple Air II, AirBeam	Can be in instruments related to the concentration of suspended particles in the air or other environmental improvement equipment	Kelly et al., (2017)* Zheng et al. (2018) Jayaratne et al. (2018) Zamora et al. (2019) Kuula et al. (2019) Bulot et al. (2020) Sayahi, Butterfield, and Kelly (2019) He, Kuerbanjiang, and Dhaniyala (2020) Badura et al. (2018)*	2	4.73	2430

Asterisks (*) indicate a different version from the manufacturer. LB: lower bound of the functional range from [Zou, Young, Chen, Liu, May & Clark \(2020\)](#). UB: upper bound of the functional range from [Zou, Young, Wickey, May & Clark \(2020\)](#). See text for details.

Table 2

Information related to the integrated devices included in this study.

Sensor	Cost (US dollars)	Communication	Sensor	Features	Previous Studies	No. of Units Tested	LB ($\mu\text{g m}^{-3}$)	UB ($\mu\text{g m}^{-3}$)
AirThinx (ID1)	\$699	Cellular, WiFi, and Bluetooth. Uses Netronix® cloud-based storage.	Plantower	Also provides CO ₂ , formaldehyde, VOC, temperature, humidity, and pressure.		1	3.44	1205
AirBeam2 (ID2)	\$249	Cellular networks, WiFi, Bluetooth, serial connector.	Plantower PMS7003	Weather resistant, AirCasting App is managed by HabitatMap, a 501(c)(3) raising awareness about the impact of the environment on human health	Sousan, Koehler, Hallett, and Peters (2017) Singer and Delp (2018) Northcross et al. (2013)	3	3.87	1184
Dylos DC1100 PRO (ID3)	\$269	Internal storage, serial connector.	Dylos	The Dylos also uses its own computer program to interpret sensor readings that are stored internally.	Williams, Kaufman, Hanley, Rice, and Garvey (2014) Steinle, Reis, and Sabel (2013) Polidori, Papapostolou, and Zhang (2016) Manikonda, Hopke, and Ferro (2016) Jiao et al. (2016)* Sousan et al. (2016)* Han et al. (2017)* Hojajji et al. (2017)	3	3.50	1020
TSI BlueSky (ID4)	\$400	Serial connector.	Plantower PMSA003 (x2)			2	4.26	1241
Purple Air II (ID5)	\$249	SD card, serial connector, and WiFi.	Plantower PMS5003 (x2)	Also provides temperature, RH, and pressure.	Polidori et al. (2016) Singer and Delp (2018) Feenstra et al. (2019) Malings et al. (2020) Tryner et al. (2020)	3	4.40	843

Asterisks (*) represent a previous version of the device. LB: lower bound of the functional range from Zou, Young, Chen, et al. (2020). UB: upper bound of the functional range from Zou, Young, Wickey, et al. (2020). See text for details.

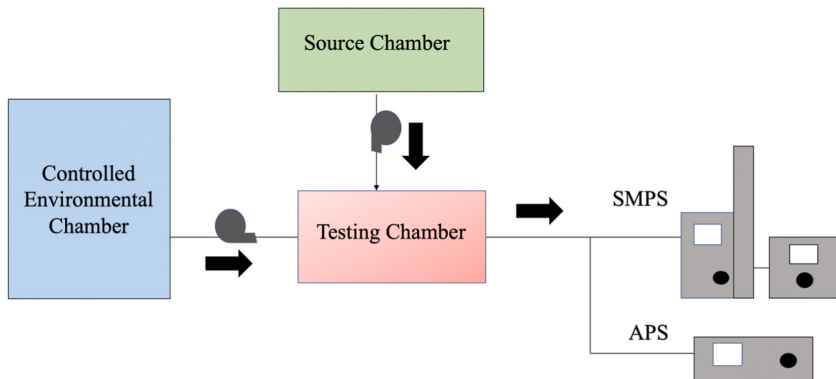


Fig. 1. Schematic of the experimental setup.

hygroscopic uptake will increase both the SMPS + APS mass concentration and the sensor mass concentration, and any differences between the two can elucidate how RH affects the sensors' response.

Temperature and RH were controlled in the testing chamber by siphoning air from an automatically controlled four cubic foot (0.11 m^3) environmental chamber (ESPEC Inc.; labeled as “Controlled Environmental Chamber” in Fig. 1) and injecting the conditioned air into the chamber housing the sensors through a pump. This was done rather than testing sensors directly in the conditioned chamber in order to prevent deposition of particles onto the evaporator and heating coils in the conditioned chamber. The flow rate of air pumped into the testing chamber from the controlled environmental chamber was set to 6 L min^{-1} via two critical orifices in order to equal the flow rate drawn by the research-grade instruments. A thermistor and thin film capacitance humidity sensor (Fisher Scientific Traceable $\pm 0.4^\circ\text{C}$, $\pm 1.5\%$ RH) were placed inside the testing chamber to record psychrometric conditions.

2.3. Experimental protocol

Twenty-five decay tests were conducted under different temperature and RH conditions, listed in Table 3. These conditions represent an optimized experimental matrix that simultaneously ensured good statistical properties in the outputs, included repeatability tests, and covered the range of conditions in which we were interested. Unlike outdoor investigations of temperature and RH effects, this optimized design resulted in temperature and RH effects that were uncorrelated.

We used incense and burnt toast smoke as two representative indoor particle sources. To generate incense particles, we used stick incense (sandalwood flavor), igniting it with a direct flame and then blowing out the flame to allow slow smoldering of the stick to produce more smoke particles. We then put the stick into the source chamber prior to transfer into the testing chamber. To generate burnt toast smoke, we used a toaster to heat the bread several times until smoke was generated and placed the toaster inside the source chamber. Once the concentration reached a high concentration (roughly $100\text{--}1000 \mu\text{g m}^{-3}$), the source was removed from the source chamber, and the particle concentration in the testing chamber was allowed to naturally decay. At the beginning of each test, we generated a high concentration of particles in yet another chamber, labeled “Source Chamber” in Fig. 1, and pumped the particle-laden air into the testing chamber. We then stopped injecting the source, and let the concentration in the chamber naturally decay (mainly via extraction of chamber air by the research-grade instruments) until all sensors' concentration reached near zero. The only sinks



Fig. 2. Photograph of interior of insulation testing chamber with sensors on racks.

Table 3

Experimental conditions for decay tests.

Run	T [°C]	RH [%]	Run	T [°C]	RH [%]	Run	T [°C]	RH [%]
1	20	40	10	30	15	19	40	30
2	30	60	11	40	30	20	25	10
3	20	60	12	35	75	21	40	40
4	30	90	13	35	45	22	40	30
5	30	30	14	20	25	23	20	25
6	30	90	15	27	75	24	15	30
7	20	90	16	30	30	25	15	20
8	22.5	75	17	40	90			
9	40	60	18	27.7	45			

within the chamber were gravitational settling, deposition on chamber walls and sensors, and removal of chamber air by the research-grade instruments. This procedure is similar to the decay tests conducted in Zou, Young, Chen, et al. (2020). Particle generation and behavior in the chamber was repeatable under similar chamber conditions. We provide one example of this in Fig. S1; while there is some noise in the mass mode particle diameter, both the estimated mass concentration and the duration of the experiment are fairly consistent.

2.4. Data analysis

Because the low-cost devices and research-grade instruments had different sampling and averaging frequencies, we averaged all data into 1-min bins to allow direct comparison between all events. SMPS and APS data were merged using the approach of Khlystov, Stanier, and Pandis (2004). We assumed a spherical shape for particles from both sources (Cheng, Bechtold, Yu, & Hung, 1995; Martins et al., 1998; Wallace, 2007). To convert SMPS + APS data to mass concentrations, we assumed that the dry density of particles generated by incense was 1.06 g cm^{-3} (Cheng et al., 1995; Singer & Delp, 2018), and toast is 0.94 g cm^{-3} (Singer & Delp, 2018). Because both of these material densities are close to that of water ($\sim 1 \text{ g cm}^{-3}$), the hygroscopic uptake of water will have negligible effects on calculated wet particle mass concentrations. That is, using a volume-mixing rule for particle density, there will be $<3\%$ difference in mixture density for aerosol water contents up to 50%.

In a previous study (Zou, Young, Chen, et al., 2020), we evaluated the functional range within which low-cost particle sensor will provide reliable data. Briefly, the lower bound (LB) of this functional range was based on a “running R^2 method” to quantify at what concentration the correlation between the research-grade instruments and the sensors degrades appreciably (threshold determined to

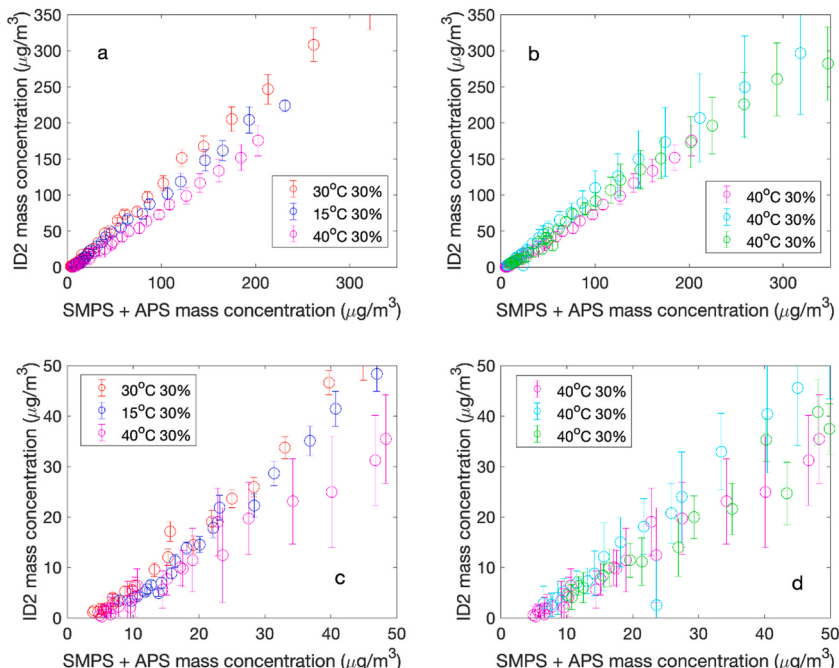


Fig. 3. Example decay tests conducted under same RH but different temperature conditions using incense as the PM sources for the three ID2 sensors. Markers represent the mean, and error bars represent the standard deviation. (For interpretation of the references to colour in this figure legend, the reader is referred to the Web version of this article.)

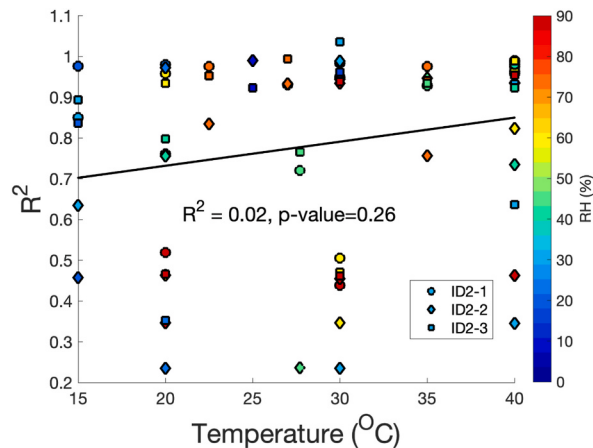


Fig. 4. The relationship between temperature and the R^2 value from linear regression of each experiment during incense decay tests for all three instances of ID2 and the research-grade instruments (SMPS + APS). The linear regression line is fit to all the slopes from three instances. (For interpretation of the references to colour in this figure legend, the reader is referred to the Web version of this article.)

be $R^2 = 0.8$). This approach is analogous to obtaining a running mean, but we fit a linear regression to the data using a window of 10 min and a step size of 1 min. The upper bound (UB) of the functional range was defined as the concentration at which the relationship between the research-grade instruments and the sensors deviates from linearity; we quantified these values using a “running slope”, and defined the UB as the concentration after which the running slope decreased for five consecutive steps. Values of both the LB and the UB for the sensors are provided in Tables 1 and 2; in this work, we truncated our data to remove values outside of this functional range.

To evaluate the effect of temperature and RH on the sensors’ outputs, we needed to establish a metric for describing accuracy. Most research on low-cost sensors evaluates sensors’ performance by comparing low-cost sensor output to that of research-grade instruments (Rai et al., 2017). Two often-used metrics are the coefficient of determination (R^2) of the linear regression between the low-cost PM sensor output and the research-grade instruments output (Karagulian et al., 2019) and the slope of this linear regression (Karagulian et al., 2019; Rai et al., 2017), both of which are used in this study. R^2 describes the correlation between the two outputs and slope provides information on the relative magnitude of the outputs.

Each slope and R^2 that we present represent one decay test using one instance of the same type of sensor and describe the relative response of the sensors to the research-grade instruments. Because both the sensors and the research-grade instruments are sampling particles that may be subject to hygroscopic growth, any effects that T or RH have on the relative response will isolate how those variables influence the sensors’ response. In the online Supporting Information (Table S1), we demonstrate that a single-variable linear regression is best model for capturing this relationship.

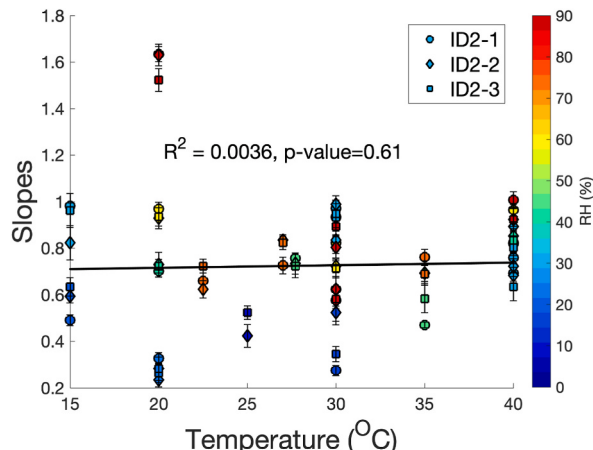


Fig. 5. The relationship between temperature and slopes from linear regression of each experiment during incense decay tests for all three instances of ID2 and the research-grade instruments (SMPS + APS). Error bars represent the standard error of the slope from linear regression. The linear regression line is fit to all the slopes from three instances. (For interpretation of the references to colour in this figure legend, the reader is referred to the Web version of this article.)

Table 4

Slope, standard error (SE), and p-values of linear regressions between temperature and R^2 or temperature and slopes from individual experiments, using incense and toast as the sources. Multiple entries for a given sensor represent different instances of that sensor.

Sensor	Incense						Toast					
	T vs. R^2			T vs. slope			T vs. R^2			T vs. slope		
	slope	SE	p-value									
ID1	0.008	0.005	0.281	0.005	0.012	0.126	0.005	0.005	0.345	0.001	0.012	0.988
ID2	0.005	0.004	0.246	0.003	0.007	0.960	0.001	0.005	0.832	0.001	0.007	0.825
	0.007	0.006	0.352	0.004	0.006	0.504	0.001	0.001	0.943	0.010	0.009	0.891
	0.005	0.005	0.165	0.001	0.006	0.827	0.002	0.001	0.901	0.008	0.008	0.903
ID3	0.009	0.004	0.065	0.002	0.005	0.788	0.007	0.008	0.268	0.005	0.009	0.593
	0.007	0.005	0.073	0.001	0.004	0.942	0.005	0.003	0.268	0.004	0.008	0.385
	0.006	0.005	0.039	-0.003	0.005	0.396	0.002	0.004	0.549	0.001	0.007	0.435
ID4	0.007	0.006	0.211	0.009	0.009	0.299	0.007	0.005	0.272	0.004	0.010	0.559
	0.003	0.004	0.235	0.016	0.010	0.096	0.001	0.001	0.136	0.001	0.011	0.867
ID5	0.007	0.007	0.100	0.021	0.012	0.078	0.004	0.005	0.634	0.001	0.015	0.963
	0.004	0.006	0.059	0.023	0.017	0.058	0.006	0.004	0.190	0.001	0.013	0.981
	0.004	0.006	0.069	0.020	0.009	0.043	0.001	0.004	0.328	0.001	0.001	0.891
BS1	0.004	0.004	0.182	0.001	0.018	0.455	0.003	0.006	0.461	0.013	0.017	0.99
	0.007	0.002	0.281	0.010	0.002	0.558	0.005	0.005	0.765	0.001	0.021	0.436
BS2	0.006	0.006	0.983	0.028	0.029	0.278	0.016	0.009	0.520	0.001	0.003	0.227
	0.003	0.004	0.948	0.010	0.018	0.404	0.007	0.007	0.379	0.003	0.002	0.879
	0.003	0.003	0.979	0.033	0.009	0.834	0.007	0.007	0.168	0.001	0.005	0.382
BS3	0.002	0.006	0.567	0.016	0.008	0.835	0.007	0.006	0.13	0.006	0.001	0.777
	0.003	0.004	0.695	0.002	0.009	0.161	0.004	0.004	0.41	0.004	0.013	0.469

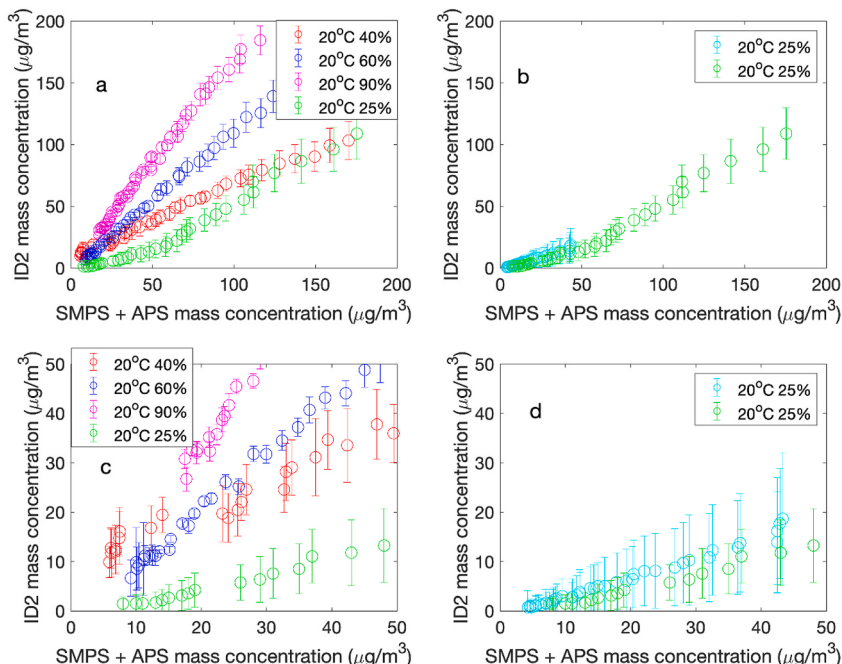


Fig. 6. Example decay tests conducted under same temperature but different RH conditions using incense as the PM sources (ID2 sensors). Markers represent the mean, and error bars represent the standard deviation. (For interpretation of the references to colour in this figure legend, the reader is referred to the Web version of this article.)

3. Results and discussion

In this section, we first present results illustrating the effect of each variable in isolation, and then we attempt to quantify the relative importance of each variable in determining sensor performance. Finally, we apply our correction algorithm to sensor outputs and assess the improvement.

Table 5

Slope, standard error (SE), and p-values of linear regressions between RH and R^2 and RH and slope using incense and toast as the particle sources. Multiple entries for a given sensor represent different instances of that sensor. Bolded p-values indicate slopes that are statistically different from zero with 99% confidence.

Sensor	Incense						Toast					
	RH vs. R^2			RH vs. slope			RH vs. R^2			RH vs. slope		
	slope	SE	p-value	slope	SE	p-value	slope	SE	p-value	slope	SE	p-value
ID1	-0.001	0.001	0.310	0.008	0.003	0.010	0.001	0.002	0.593	0.015	0.003	1.5e-5
ID2	-0.002	0.002	0.950	0.005	0.002	0.003	0.001	0.001	0.722	0.008	0.002	1.4e-4
	-0.001	0.002	0.203	0.005	0.001	0.008	0.001	0.001	0.836	0.014	0.001	3.8e-4
	-0.001	0.002	0.832	0.001	0.002	0.010	-0.001	0.001	0.635	0.010	0.002	5.0e-5
ID3	-0.001	0.002	0.990	-0.001	0.002	0.575	0.001	0.003	0.834	0.007	0.002	5.0e-4
	0.003	0.001	0.832	-0.001	0.001	0.623	0.001	0.001	0.938	0.004	0.003	0.008
	0.002	0.002	0.037	-0.001	0.001	0.452	-0.001	0.001	0.539	0.012	0.003	0.006
ID4	0.001	0.002	0.391	0.008	0.002	0.025	0.001	0.002	0.429	0.014	0.004	4.1e-4
	0.001	0.002	0.132	0.009	0.003	0.015	-0.001	0.001	0.643	0.017	0.004	1.3e-4
ID5	-0.001	0.002	0.623	0.011	0.003	0.036	0.001	0.001	0.864	0.015	0.004	1.6e-4
	-0.001	0.001	0.894	0.010	0.003	0.002	0.001	0.002	0.471	0.013	0.001	1.0e-4
	0.001	0.001	0.559	0.010	0.002	0.007	-0.001	0.002	0.792	0.020	0.004	2.8e-4
BS1	-0.001	0.001	0.469	0.001	0.001	0.024	-0.002	0.002	0.956	0.002	0.005	1.9e-4
	-0.001	0.002	0.963	0.011	0.005	0.036	0.001	0.001	0.992	0.021	0.001	0.008
BS2	-0.001	0.002	0.990	0.012	0.008	0.032	0.003	0.003	0.265	0.004	0.001	0.006
	0.001	0.002	0.981	0.023	0.005	0.052	0.002	0.003	0.483	0.002	0.002	0.007
	0.001	0.001	0.879	0.007	0.003	0.012	-0.001	0.002	0.167	0.002	0.001	0.004
BS3	-0.001	0.001	0.962	0.008	0.002	0.007	-0.001	0.002	0.990	0.012	0.003	2.1e-4
	0.001	0.002	0.932	0.009	0.002	0.008	0.001	0.001	0.981	0.014	0.004	0.006

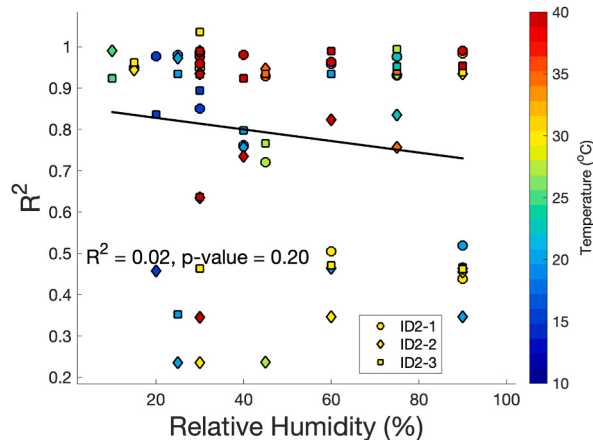


Fig. 7. The relationship between RH and the R^2 value from linear regression of each experiment during incense decay tests for all three instances of ID2 and the research-grade instruments (SMPS + APS). The linear regression line is fit to all the slopes from three instances. (For interpretation of the references to colour in this figure legend, the reader is referred to the Web version of this article.)

3.1. Temperature effects on sensor performance

In Fig. 3, we show an illustrative example of the response of one sensor (ID2) to incense during four decay tests under the same RH but different temperature conditions (panel a) and three repeated trials at 40 °C and 30% RH (panel b). The markers represent the average across three instances of this sensor, and the error bars represent the standard deviation among different instances of the same sensor. We highlight two features of Fig. 3 that are generally true for most sensors tested:

1. Results of repetitions of experimental conditions track each other well (Fig. 3b).
2. There is an apparent difference in data at different temperatures, but the results for one temperature for a given sensor type typically falls within one standard deviation of the results for other temperatures, suggesting temperature may not be a significant determining variable for sensor output (Fig. 3a).

In order to quantify this second conclusion, we fit a linear regression to data from each experiment to obtain the slope and R^2 for that particular experiment (i.e., one combination of temperature and RH from Table 3). We then regressed 1) the slopes of all

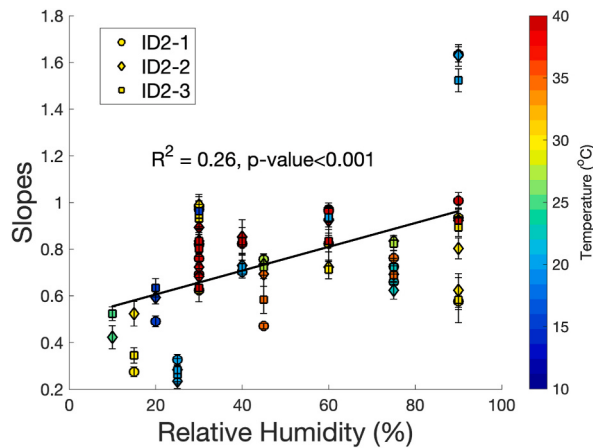


Fig. 8. The relationship between RH and slopes from linear regression of each experiment during incense decay tests for all three instances of ID2 and the research-grade instruments (SMPS + APS). Error bars represent the standard error of the slope from linear regression. The linear regression line is fit to all the slopes from three instances. (For interpretation of the references to colour in this figure legend, the reader is referred to the Web version of this article.)

experiments and 2) the R^2 values of all experiments to the temperatures at which they were performed, to determine if temperature had a significant effect on slope or R^2 across the different experiments. An example of this is provided in Figs. 4 and 5 for ID2 using incense as the particle source. In Figs. 4 and 5, individual points are the R^2 and slope values (y-axis), respectively, from each experiment, as a function of the temperature at which the experiment was conducted (x-axis). The markers in Figs. 4 and 5 are color-coded by RH.

The p-value of the resulting linear model shown in Fig. 4 is 0.26 and its R^2 is practically zero, indicating very low confidence that effect of temperature on the sensors' correlation to the research-grade instruments is distinguishable from pure chance. We show similar results for all sensors tested in Table 4; only one instance of one sensor (ID3) using incense as the particle source exhibited a relationship between temperature and sensor correlation to research-grade instruments with 95% confidence or greater.

In Fig. 5, we show the results of similar hypothesis testing for the effect of temperature on slope of the linear regression between low-cost sensor output and that of research-grade instruments. Again, although there is an apparent increasing trend in the derived slopes with increasing temperature, the p-value (0.61) suggests that this is not significantly different from zero. Table 4 shows that this

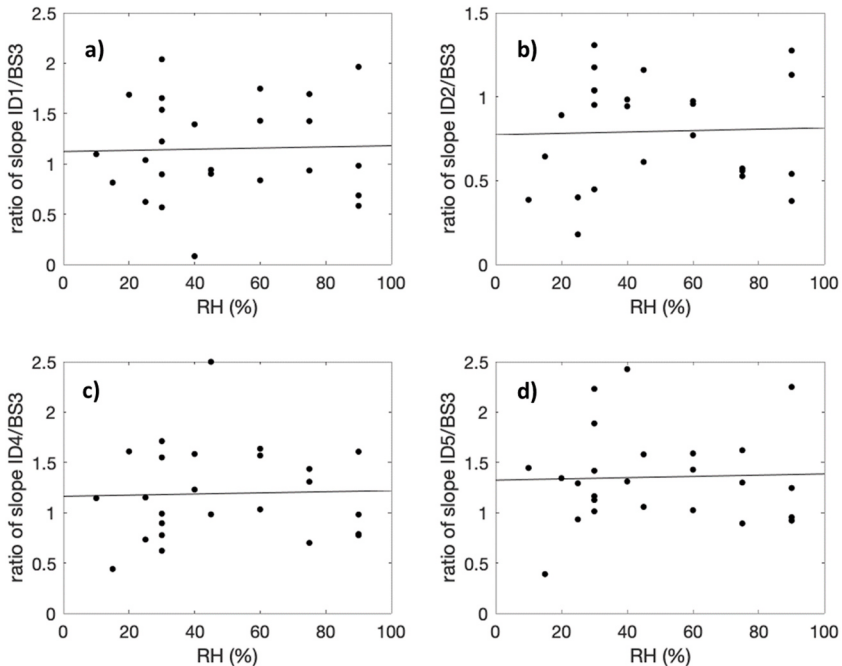


Fig. 9. The relationship of the ratio of slopes between the integrated devices containing a Plantower sensor and the bare Plantower 5003 sensor (BS3) as a function of RH: a) ID1; b) ID2; c) ID4; and d) ID5. Note the different scales on the y-axes.

holds for all sensors tested, with the exception of one instance of ID5 using incense as the particle source, implying the effect of temperature on the magnitude of a low-cost particle sensor's response relative to the research-grade instruments is negligible. From these experiments, we do not find a compelling reason to assert any relationship between low cost sensor output and temperature. This finding of no temperature effect is consistent with previous studies, which considered other low-cost particle sensors (Holstius, Pilisetti, Smith, & Seto, 2014; Jiao et al., 2016; Wang et al., 2015; Williams, Kaufman, Hanley, Rice, & Garvey, 2015), and it provides an independent confirmation of the stability of the Plantower sensor, in agreement with its specification sheet.

3.2. RH effects on sensor performance

In Fig. 6, we present results analogous to those in Fig. 3, but with fixed temperature (at 20 °C) and varying RH between experiments, with two repeated trials at 25% RH in Fig. 6b. Unlike in Fig. 3, the differences between different experiments do not appear to agree within measurement uncertainty: the experiments at 90% RH had the greatest slope, followed by 60% RH, 40% RH, and 25% RH. These results in Fig. 6 are an exemplary case in that the slopes of the curves monotonically increase with RH. This is not the case for all sensors, but for every sensor except ID3, there appears to be a positive bias on the relative response of the sensors as RH increases (see Table 5, Tables S2–S7, and Figs. S2–S14). Because we did not dry the particles prior to sampling by the research-grade instruments, this bias appears to be beyond what would be expected for hygroscopic particle growth alone.

Similar to the temperature experiments, we also evaluated how RH affects sensor performance by considering the relationship of RH to slope and R². Example results are shown in Figs. 7 and 8, and Table 5 provides a summary across all sensors. Fig. 7 demonstrates the relationship between RH and R² for ID2 and suggests there is no statistically significant relationship between the RH and R² (p-values are all greater than 0.01) for this sensor. This trend holds true for all sensors tested (Table 5), with a single exception of one instance of one sensor (ID3) for one particular source (incense), which may indicate a problem with that one specific instance of that sensor. This suggests that although several previous works have shown a relationship between sensor performance and RH conditions, the correlation to research-grade instruments outputs does not seem to be significantly affected for the sensors and conditions tested.

We sought to clarify this further by looking at not just the correlation, but the magnitude of the low-cost sensor response, as quantified by the slope of the regression between the sensor signal and that of the research-grade instruments. Interestingly, as shown in Fig. 8, RH has a clear, statistically-significant effect (p-value < 0.01) on the slope of the regression line between ID2 and the research-grade instruments for incense as the particle source. That is, the relative response between the sensor and the research-grade instruments increased with increasing RH. This finding is roughly consistent with previous studies, that demonstrate an increase to a sensor's output with increasing RH (Badura et al., 2018; Bulot et al., 2019, 2020; Han et al., 2017; Jayaratne et al., 2018; Zamora et al., 2019; Liu et al., 2019; Morawska et al., 2018; Mukherjee et al., 2019; Tryner et al., 2020; Wang et al., 2015). Of these, only Bulot et al. (2020) considered the slope between the sensors and a TSI DustTrak DRX 8533 with varying RH; however, they did not quantify any trends in the slope. Qualitatively, there does not appear to be a relationship between those slopes and RH, likely because the DustTrak, like many low-cost particle sensors, is a nephelometer, in that it uses aerosol light scattering to quantify particle mass concentrations.

Interestingly, the relative response of most sensors tested had a statistically significant increase with increasing RH. Results shown in Table 5 suggest that all slopes are statistically different from zero at a 99% confidence level for toast smoke, while all slopes are statistically different from zero at a 95% confidence level for incense (except for ID3). Because the sensors and the research-grade instruments are both sampling wet particles, hygroscopic growth will affect both sets of measurements, which may be a physical explanation for why our model selection in Section S1 suggests that a linear model is the most appropriate.

Of the mechanisms outlined by Badura et al. (2018), the effect that RH has on water uptake, and therefore, on the complex refractive index of the particles may be the most plausible. We expect that both incense and toast smoke will contain some light-absorbing carbon. Therefore, as the particles grow due to hygroscopic uptake of water, they will become relatively less absorbing at the sensors' wavelengths of light, as the relative abundance of absorbing material will decrease. For example, Hagan and Kroll (2020) demonstrate that as particles become less absorbing, they become less biased (cf., their Fig. 4). Hence, the observed differences between toast smoke and incense may be related to the hygroscopicity of the particles; we do note that this is purely speculative, so we do not elaborate further.

3.3. Variability between sensors, sources, and repeated experiments

Our matrix of sensors combined with two particle sources and some repeated experimental conditions enables the investigation of variability in the relative response of the sensors to the research-grade instruments.

3.3.1. Variability between experimental conditions

To investigate the cause of the variability among experiments, we conducted an n-way analysis of variance (ANOVA) using input values from Tables S2 and S5. Our independent variables were the sensor used, the particle source, temperature, and RH. We then calculated the proportion of variance (ω^2):

$$\omega^2 = \frac{SSB - (a - 1)MSE}{SST + MSE} \quad Eq. 1$$

where SSB is the sum of squares due to a given independent variable, a is the number of independent variables, MSE is the mean square error, and SST is the total sum of squares. Results of this analysis suggest that the sensor model, particle source, temperature, and RH

accounted for 15.2%, 4.7%, 5.3%, and 11.1% of the variability, respectively.

These n-way ANOVA results suggest that the type of sensor used has the largest contribution to overall variance in our results, suggesting that although the sensors are all nephelometers, the form factor, wavelength of light, processing algorithm, and other “operating” differences can result in large variability. The results for RH and particle source are consistent with our previous results, suggesting that variations in the sensors’ response can occur as RH varies or as the particle source varies. Variations in temperature account for roughly 5% of the variability in the slopes, which is inconsistent with our results in, e.g., Fig. 5; however, there is some noise in, e.g., Fig. 8, for a given RH. Therefore, temperature may account for a small, yet statistically insignificant, role in affecting the sensors’ outputs.

3.3.2. Variability in repeated experiments

To quantify differences between repeated temperature and RH pairs (e.g., Experiments 14 and 23 in Table 1), we calculated the relative difference in the slopes for each sensor if there were two replicates or the relative standard deviation between the slopes if experiments were conducted in triplicate. These results are presented in Table S8, separated by particle source. Generally, the results are more stable when temperature < 40 °C, which could be related to the fact that the sensor manufacturers tend to report 40 °C as the upper bound of the sensors’ working temperature; this fact could also contribute to the fractional variance for temperature in our n-way ANOVA results.

Some of this variability may be related to instance-to-instance variability for a given sensor, which can be estimated using results from Tables S2-S3 and S5-S6. For example, ID3 tends to have high variability in Table S8, and it also tends to have high “relative standard error” for both incense and toast smoke. In fact, we identified both ID3 and BS2 as having lower “manufacturer consistency” in previous work (Zou, Young, Wickey, et al., 2020). This instance-to-instance variability may also be part of the explanation for the large fraction of “random” error in our n-way ANOVA (i.e., the error that cannot be explained by our independent variables).

3.3.3. Variability in plantower-based sensors

Because four of our integrated devices incorporated some version of a Plantower sensor (ID1, ID2, ID4, and ID5), we investigated whether there were any systematic trends between those devices and BS3. To visualize this, we present the ratio of the slope from an integrated device to the slope from the bare sensor for a given experiment in Fig. 9. Qualitatively, there is considerable noise among individual experiments (markers in the figure). To quantify these differences, we conducted significance testing. None of the slopes of the best-fit lines shown in the figure were significantly different from zero at a 99% confidence level. We also tested the mean values of the ratios presented in Fig. 9 to determine if they were significantly different from unity. For ID1 and ID4, these means were not significantly different from unity at a 99% confidence level; however, for ID2 and ID5, they were significantly different. Consequently, our data suggests that while different form factors and proprietary algorithms can result in discrepancies between these Plantower-based sensors, but none of them appears to be disproportionately influenced by RH, relative to each other.

4. Conclusion

In this study we conducted an optimized matrix of twenty-five decay tests under different temperature and RH conditions using two common challenge sources and simultaneous measurement with research-grade instruments. Analysis of results showed a few interesting results:

- 1) No statistically significant relationship between temperature and low-cost sensor output emerged for any sensor tested in the range of 15 °C – 40 °C, suggesting this variable is not a large contributor to sensor performance degradation for indoor environments and likely does not need to be taken into consideration. This is largely in line with previous research on the subject.
- 2) Similarly, no significant relationship between the correlation of low-cost sensor output and humidity emerged from the tests conducted in the range of 10% – 90%. This suggests that while the magnitude of sensor output may change with humidity, the signal remains correlated to that of research-grade instruments and a simple calibration may improve performance.
- 3) There is a significant linear relationship between RH and the relative response of the low-cost particle sensors. This may be related to changes in the particles’ complex refractive index as hygroscopic growth occurs, thus affecting the light-scattering measurements by the low-cost sensors.
- 4) In our n-way ANOVA, the sensor model appears to be the largest source of variability, implying that sensors produced by different manufacturers perform differently. Moreover, the agreement between the Plantower-based sensors (ID1, ID2, ID4, ID5, and BS3) is variable; however, none of these sensors are disproportionately affected by variations in RH.

Declaration of competing interest

The authors declare that they have no known competing financial interests or personal relationships that could have appeared to influence the work reported in this paper.

Acknowledgements

This work was funded by ASHRAE (RP-1756). The authors thank the editor, Dr. Kerry Kelly, and two anonymous reviewers for constructive feedback.

Appendix A. Supplementary data

Supplementary data to this article can be found online at <https://doi.org/10.1016/j.jaerosci.2020.105715>.

References

- Badura, M., Batog, P., Drzeniecka-Osiadacz, A., & Modzel, P. (2018). Evaluation of low-cost sensors for ambient PM_{2.5} monitoring. *Journal of Sensors*. <https://doi.org/10.1155/2018/5096540>. 2018.
- Budde, M., El Masri, R., Riedel, T., & Beigl, M. (2013). Enabling low-cost particulate matter measurement for participatory sensing scenarios. In *Proceedings of the 12th international conference on mobile and ubiquitous multimedia - MUM '13* (pp. 1–10). New York, New York, USA: ACM Press. <https://doi.org/10.1145/2541831.2541859>.
- Bulot, F. M. J., Johnston, S. J., Basford, P. J., Easton, N. H. C., Apetroae-Cristea, M., Foster, G. L., ... Loxham, M. (2019). Long-term field comparison of multiple low-cost particulate matter sensors in an outdoor urban environment. *Scientific Reports*, 9(1), 1–13. <https://doi.org/10.1038/s41598-019-43716-3>
- Bulot, F. M. J., Russell, H. S., Rezaei, M., Johnson, M. S., Ossont, S. J. J., Morris, A. K. R., ... Cox, S. J. (2020). Laboratory comparison of low-cost particulate matter sensors to measure transient events of pollution. *Sensors*, 20(8), 2219. <https://doi.org/10.3390/s20082219>
- Cheng, Y. S., Bechtold, W. E., Yu, C. C., & Hung, I. F. (1995). Incense smoke: Characterization and dynamics in indoor environments. *Aerosol Science and Technology*, 23(3), 271–281. <https://doi.org/10.1080/02786829508965312>
- Crilley, L. R., Shaw, M., Pound, R., Kramer, L. J., Price, R., Young, S., ... Pope, F. D. (2018). Evaluation of a low-cost optical particle counter (Alphasense OPC-N2) for ambient air monitoring. *Atmospheric Measurement Techniques*, 11(2), 709–720. <https://doi.org/10.5194/amt-11-709-2018>
- Feeenstra, B., Papapostolou, V., Hasheminassab, S., Zhang, H., Boghossian, B., Der, Cocker, D., et al. (2019). Performance evaluation of twelve low-cost PM_{2.5} sensors at an ambient air monitoring site. *Atmospheric Environment*, 216, 116946. <https://doi.org/10.1016/j.atmosenv.2019.116946>
- Hagan, D. H., & Kroll, J. H. (2020). Assessing the accuracy of low-cost optical particle sensors using a physics-based approach. *Atmospheric Measurement Techniques Discussions*. <https://doi.org/10.5194/amt-2020-188>
- Han, I., Symanski, E., & Stock, T. H. (2017). Feasibility of using low-cost portable particle monitors for measurement of fine and coarse particulate matter in urban ambient air. *Journal of the Air and Waste Management Association*, 67(3), 330–340. <https://doi.org/10.1080/10962247.2016.1241195>
- He, M., Kuerbanjiang, N., & Dhaniyala, S. (2020). Performance characteristics of the low-cost Plantower PMS optical sensor. *Aerosol Science and Technology*, 54(2), 232–241. <https://doi.org/10.1080/02786826.2019.1696015>
- Hojaiji, H., Kalantarian, H., Bui, A. A. T., King, C. E., & Sarrafzadeh, M. (2017). Temperature and humidity calibration of a low-cost wireless dust sensor for real-time monitoring. In , Vols. 1–6. *IEEE sensors applications symposium, proceedings*. <https://doi.org/10.1109/SAS.2017.7894056>. SAS 2017 - 2017.
- Holstius, D. M., Pillarisetti, A., Smith, K. R., & Seto, E. (2014). Field calibrations of a low-cost aerosol sensor at a regulatory monitoring site in California. *Atmospheric Measurement Techniques*, 7(4), 1121–1131. <https://doi.org/10.5194/amt-7-1121-2014>
- Jayaratne, R., Liu, X., Thai, P., Dunabin, M., & Morawska, L. (2018). The influence of humidity on the performance of a low-cost air particle mass sensor and the effect of atmospheric fog. *Atmospheric Measurement Techniques*, 11(8), 4883–4890. <https://doi.org/10.5194/amt-11-4883-2018>
- Jiao, W., Hagler, G., Williams, R., Sharpe, R., Brown, R., Garver, D., ... Buckley, K. (2016). Community Air Sensor Network (CAIRSENSE) project: Evaluation of low-cost sensor performance in a suburban environment in the southeastern United States. *Atmospheric Measurement Techniques*, 9(11), 5281–5292. <https://doi.org/10.5194/amt-9-5281-2016>
- Karagulian, F., Barbiere, M., Kotsev, A., Spinelle, L., Gerboles, M., Lagler, F., ... Borowiak, A. (2019). Review of the performance of low-cost sensors for air quality monitoring. *Atmosphere*, 10(9). <https://doi.org/10.3390/atmos10090506>
- Kelly, K. E., Whitaker, J., Petty, A., Widmer, C., Dybwad, A., Sleeth, D., ... Butterfield, A. (2017). Ambient and laboratory evaluation of a low-cost particulate matter sensor. *Environmental Pollution*, 221, 491–500. <https://doi.org/10.1016/j.envpol.2016.12.039>
- Khlystov, A., Stanier, C., & Pandis, S. N. (2004). An algorithm for combining electrical mobility and aerodynamic size distributions data when measuring ambient aerosol. *Aerosol Science and Technology*, 38(SUPPL. 1), 229–238. <https://doi.org/10.1080/02786820390229543>
- Klepeis, Neil, Nelson, William, Ott, Wayne, Robinson, John, Tsang, Andy, Switzer, Paul, & Engelmann, William (2001). The National Human Activity Pattern Survey (NHAPS): A Resource for Assessing Exposure to Environmental Pollutants. *Journal of Exposure Science & Environmental Epidemiology*, 11(3), 231–252. <https://doi.org/10.1038/sj.jea.7500165>
- Kuula, J., Mäkelä, T., Aurela, M., Teinilä, K., Varjonen, S., Gonzales, O., et al. (2019). Laboratory evaluation of particle size-selectivity of optical low-cost particulate matter sensors. *Atmospheric Measurement Techniques Discussions*, (December), 1–21. <https://doi.org/10.5194/amt-2019-422>
- Liu, H. Y., Schneidner, P., Haugen, R., & Vogt, M. (2019). Performance assessment of a low-cost PM 2.5 sensor for a near four-month period in Oslo, Norway. *Atmosphere*, 10(2), 1–19. <https://doi.org/10.3390/atmos10020041>
- Li, Zhisheng, Wen, Qingmei, & Zhang, Ruilin (2017). Sources, health effects and control strategies of indoor fine particulate matter (PM_{2.5}): A review. *Science of The Total Environment*, 586, 610–622. <https://doi.org/10.1016/j.scitotenv.2017.02.029>
- Liu, D., Zhang, Q., Jiang, J., & Chen, D. R. (2017). Performance calibration of low-cost and portable particulate matter (PM) sensors. *Journal of Aerosol Science*, 112 (May), 1–10. <https://doi.org/10.1016/j.jaerosci.2017.05.011>
- Malings, C., Tanzer, R., Hauryliuk, A., Saha, P. K., Robinson, A. L., Presto, A. A., et al. (2020). Fine particle mass monitoring with low-cost sensors: Corrections and long-term performance evaluation. *Aerosol Science and Technology*, 54(2), 160–174. <https://doi.org/10.1080/02786826.2019.1623863>
- Manikonda, A., Hopke, P. K., & Ferro, A. R. (2016). *Laboratory assessment of low-cost PM monitors* (vol. 102, pp. 29–40). <https://doi.org/10.1016/j.jaerosci.2016.08.010>
- Martins, J. V., Artaxo, P., Liousse, C., Reid, J. S., Hobbs, P. V., & Kaufman, Y. J. (1998). Effects of black carbon content, particle size, and mixing on light absorption by aerosols from biomass burning in Brazil. *Journal of Geophysical Research: Atmospheres*, 103(D24), 32041–32050. <https://doi.org/10.1029/98JD02593>
- Morawska, L., Thai, P. K., Liu, X., Asumadu-sakyi, A., Ayoko, G., Bartonova, A., ... Williams, R. (2018). Applications of low-cost sensing technologies for air quality monitoring and exposure assessment : How far have they gone ? . <https://doi.org/10.1016/j.envint.2018.04.018>, 116, February, 286–299.
- Mukherjee, A., Brown, S. G., McCarthy, M. C., Pavlovic, N. R., Stanton, L. G., Snyder, J. L., ... Hafner, H. R. (2019). *Network of low-cost sensors*.
- Northcross, A. L., Edwards, R. J., Johnson, M. A., Wang, Z. M., Zhu, K., Allen, T., et al. (2013). A low-cost particle counter as a realtime fine-particle mass monitor. *Environmental Sciences: Processes and Impacts*, 15(2), 433–439. <https://doi.org/10.1055/s-0035-1545797>
- Polidori, A., Papapostolou, V., & Zhang, H. (2016). *Laboratory evaluation of low-cost air quality sensors* (August).
- Rai, A. C., Kumar, P., Pilla, F., Skouloudis, A. N., Di Sabatino, S., Ratti, C., ... Rickerby, D. (2017). End-user perspective of low-cost sensors for outdoor air pollution monitoring. *The Science of the Total Environment*, 607(608), 691–705. <https://doi.org/10.1016/j.scitotenv.2017.06.266>
- Sayahi, T., Butterfield, A., & Kelly, K. E. (2019). Long-term field evaluation of the Plantower PMS low-cost particulate matter sensors. *Environmental Pollution*, 245, 932–940. <https://doi.org/10.1016/j.envpol.2018.11.065>
- Singer, B. C., & Delp, W. W. (2018). Response of consumer and research grade indoor air quality monitors to residential sources of fine particles. *Indoor Air*, 28(4), 624–639. <https://doi.org/10.1111/ina.12463>
- Sousan, K., Koehler, K., Hallett, L., & Peters, T. M. (2016). Evaluation of the Alphasense optical particle counter (OPC-N2) and the Grimm portable aerosol spectrometer (PAS-1.108). *Aerosol Science and Technology*, 50(12), 1352–1365. <https://doi.org/10.1080/02786826.2016.1232859>
- Sousan, S., Koehler, K., Hallett, L., & Peters, T. M. (2017). Evaluation of consumer monitors to measure particulate matter. *Journal of Aerosol Science*, 107, 123–133. <https://doi.org/10.1016/j.jaerosci.2017.02.013>

- Steinle, S., Reis, S., & Sabel, C. E. (2013). Quantifying human exposure to air pollution-Moving from static monitoring to spatio-temporally resolved personal exposure assessment. *The Science of the Total Environment*, 443, 184–193. <https://doi.org/10.1016/j.scitotenv.2012.10.098>
- Tryner, J., L'Orange, C., Mehaffy, J., Miller-Lionberg, D., Hofstetter, J. C., Wilson, A., et al. (2020). Laboratory evaluation of low-cost PurpleAir PM monitors and in-field correction using co-located portable filter samplers. *Atmospheric Environment*, 220, 117067. <https://doi.org/10.1016/j.atmosenv.2019.117067>. June 2019.
- Wallace, L. (2007). Indoor sources of ultrafine and accumulation mode Particles : Size distributions , size-resolved concentrations , and source strengths indoor sources of ultrafine and accumulation mode Particles : Size distributions. *Size-Resolved Concentrations*, 6826. <https://doi.org/10.1080/02786820600612250>
- Wang, Y., Li, J., Jing, H., Zhang, Q., Jiang, J., & Biswas, P. (2015). Laboratory evaluation and calibration of three low-cost particle sensors for particulate matter measurement. *Aerosol Science and Technology*, 49(11), 1063–1077. <https://doi.org/10.1080/02786826.2015.1100710>
- Weekly, K., Rim, D., Zhang, L., Bayen, A. M., Nazaroff, W. W., & Spanos, C. J. (2013). Low-cost coarse airborne particulate matter sensing for indoor occupancy detection. In *IEEE international conference on automation science and engineering* (pp. 32–37). <https://doi.org/10.1109/CoASE.2013.6653970>
- Williams, R., Kaufman, A., Hanley, T., Rice, J., & Garvey, S. (2014). Evaluation of field-deployed low cost PM sensors (EPA/600/R-14/464) (p. 76). United States Environmental Protection Agency. https://cfpub.epa.gov/si/si_public_record_report.cfm?Lab=NERL&dirEntryId=297517
- Williams, R., Kaufman, A., Hanley, T., Rice, J., & Garvey, S. (2015). *Evaluation of elm and speck sensors* (November).
- Zamora, M. L., Xiong, F., Gentner, D., Kerkez, B., Kohrman-Glaser, J., & Koehler, K. (2019). Field and laboratory evaluations of the low-cost planttower particulate matter sensor. *Environmental Science and Technology*, 53(2), 838–849. <https://doi.org/10.1021/acs.est.8b05174>
- Zheng, T., Bergin, M. H., Johnson, K. K., Tripathi, S. N., Shirodkar, S., Landis, M. S., ... Carlson, D. E. (2018). Field evaluation of low-cost particulate matter sensors in high-and low-concentration environments. *Atmospheric Measurement Techniques*, 11(8), 4823–4846. <https://doi.org/10.5194/amt-11-4823-2018>
- Zou, Y., Young, M., Chen, J., Liu, J., May, A., & Clark, J. D. (2020). Examining the functional range of commercially available low-cost airborne particle sensors and consequences for monitoring of indoor air quality in residences. *Indoor Air*, 30(2), 213–234. <https://doi.org/10.1111/ina.12621>
- Zou, Y., Young, M., Wickey, M., May, A., & Clark, J. D. (2020). Response of eight low-cost particle sensors and consumer devices to typical indoor emission events in a real home (ASHRAE 1756-RP). *Science and Technology for the Built Environment*, 26(2), 237–249. <https://doi.org/10.1080/23744731.2019.1676094>